Parkinsonism and Related Disorders 66 (2019) 182–188

Contents lists available at ScienceDirect

Parkinsonism and Related Disorders

journal homepage: www.elsevier.com/locate/parkreldis

Extensive cerebellar and thalamic degeneration in spinocerebellar ataxia type 10

Carlos R. Hernandez-Castillo[a], Rosalinda Diaz[b], Israel Vaca-Palomares[c], Diana L. Torres[b], Amanda Chirino[b], Aurelio Campos-Romo[d], Adriana Ochoa[e], Astrid Rasmussen[f,g], Juan Fernandez-Ruiz[b,h,*]

[a] CONACYT - Instituto de Neuroetología, Universidad Veracruzana, Veracruz, Mexico
[b] Laboratorio de Neuropsicología, Departamento de Fisiología, Facultad de Medicina, Universidad Nacional Autónoma de México, CDMX, Mexico
[c] Ciencias Cognitivas y del Comportamiento, Facultad de Psicología, Universidad Nacional Autónoma de México, CDMX, Mexico
[d] Unidad Periférica de Neurociencias, Facultad de Medicina, Universidad Nacional Autónoma de México, Instituto Nacional de Neurología y Neurocirugía "MVS", Mexico
[e] Departamento de Neurogenética, Instituto Nacional de Neurología y Neurocirugía Manuel Velasco Suárez, CDMX, Mexico
[f] Oklahoma Medical Research Foundation, Oklahoma City, OK, USA
[g] Unidad de Biología Molecular y Medicina Genómica, Instituto Nacional de Ciencias Médicas y Nutrición Salvador Zubirán, CDMX, Mexico
[h] Facultad de Psicología, Universidad Veracruzana, Xalapa, Mexico

ARTICLE INFO

Keywords:
SCA10
Voxel based morphometry
Thalamus
Seizures
Cerebellum

ABSTRACT

Introduction: Spinocerebellar ataxia type 10 (SCA10) is a hereditary neurodegenerative disorder caused by repeat expansions in the *ATXN10* gene. Patients present with cerebellar ataxia frequently accompanied by seizures. Even though loss of cerebellar Purkinje neurons has been described, its brain degeneration pattern is unknown. Our aim was to characterize the gray and white matter degeneration patterns in SCA10 patients and the association with clinical features.

Methods: We enrolled 18 patients with molecular diagnosis of SCA10 and 18 healthy individuals matched for age and sex. All participants underwent brain MRI including high-resolution anatomical and diffusion images. Whole-brain Tract-Based Spatial Statistics (TBSS) and Voxel-Based Morphometry (VBM) were performed to identify white and grey matter degeneration respectively. A second analysis in the cerebellum identified the unbiased pattern of degeneration. Motor impairment was assessed using the SARA Scale.

Results: TBSS analysis in the patient group revealed white matter atrophy exclusively in the cerebellum. VBM analysis showed extensive grey matter degeneration in the cerebellum, brainstem, thalamus, and putamen. Significant associations between cerebellar degeneration and SARA scores were found. Additionally, degeneration in thalamic GM and WM in the cerebellar lobule VI were significantly associated with the presence of seizures.

Conclusion: The results show that besides cerebellum and brainstem, brain degeneration in SCA10 includes predominantly the putamen and thalamus; involvement of the latter is strongly associated with seizures. Analysis of the unbiased degeneration pattern in the cerebellum suggests lobules VIIIb, IX, and X as the primary cerebellar targets of the disease, which expands to the anterior lobe in later stages.

1. Introduction

Spinocerebellar ataxia type 10 (SCA10) is an autosomal dominant ataxia caused by the expansion of an ATTCT pentanucleotide repeat within the coding region of *ATXN1* [1]. In SCA10 patients the nucleotide repeat is polymorphic in the range of 800–4500 ATTCT repeats, while 10 to 29 repeats are considered normal alleles. The first clinical descriptions of SCA10 were in families of Mexican ancestry [2], and subsequent studies pointed to Latin America as the region with the highest incidence [3,4]. However, subsequent investigations have shown evidence of SCA10 patients with different origins such as North America, and East Asia [5,6]. In the same way than other spinocerebellar ataxias (SCAs), SCA10 is characterized by slowly progressive cerebellar dysfunction such as limb and gait ataxia, dysarthria and ocular disturbances. The first sign of the disease is usually unbalanced gait and stance with a variable degree of limb ataxia, which is

* Corresponding author. Departamento de Fisiología, Facultad de Medicina, Universidad Nacional Autónoma de México, UNAM, Coyoacán, CDMX, Mexico.
E-mail address: jfr@unam.mx (J. Fernandez-Ruiz).

https://doi.org/10.1016/j.parkreldis.2019.08.011
Received 29 May 2019; Received in revised form 9 August 2019; Accepted 19 August 2019

characterized by jerky or uncoordinated movements unexplained by motor weakness or sensory loss [4]. The clinical diagnosis of SCA10 is mainly driven by the combination of ataxia and epileptic seizures, most often generalized motor seizures and complex partial seizures. The presence of seizures, however, is not generalizable to all SCA10 patients, e.g. in Mexican cohorts the overall prevalence of seizures is around 72% [2,4], but the rate of seizures can be as high as 100% in Peru [7] and Argentina [3], or very rare (~3.75%), as is the case in Southern Brazil [4,8–10]. Furthermore, it should be noted that seizures can also be present in other SCA subtypes, such as SCA17 and DRPLA [11] increasing the difficulty of diagnosis based solely on clinical features. Similarly, when SCA10 patients present with pure cerebellar ataxia without seizures, the etiologic diagnosis may be challenging given the many shared clinical features with the other SCAs. Thus, genetic testing for the ATTCT repeat expansion in the *ATXN10* gene is needed as a confirmatory test.

Neuropathological and neuroimaging studies on the neurodegeneration pattern in SCA10 are scarce. There is currently only one post-mortem study on SCA10 showing Purkinje cell loss as the main brain pathology in this disease [5]. Neuroimaging techniques are powerful tools in the assessment of degeneration in neurological disorders including SCAs [5]. Few studies have made radiological descriptions of MRI features of SCA10, confirming the original report of vermian and hemispheric cerebellar atrophy by visual inspection of the MRI in 8 patients [2,6,8]. However, no systematic imaging studies have been conducted to investigate the extent of SCA10-related neurodegeneration and how it affects specific areas in the whole brain. In particular, there is no information about the extent of cortical and subcortical damage resulting from the disease, and its possible correlation with the clinical phenotype. The purpose of this study is to provide a systematic characterization of the grey and white matter structural degeneration in a cohort of SCA10 patients. Hence, we used Voxel-Based Morphometry (VBM) and Tract-Based Spatial Statistics (TBSS) of the cerebral grey matter degeneration and the white matter integrity degradation in a cohort of Mexican SCA10 patients. Using a novel technique, we also analyzed the unbiased degeneration patterns of cerebellar grey matter [12]. Our approach has a dual-prong advantage in comparison to previous studies: the added power of systematic group analyzes and the possibility of removing individual variability of the degeneration patterns which are biased by the stage of the disease. The resulting pattern of degeneration points to a spatial location that is present in all the patients and possibly the primary target of the mutation. The specific configuration of the degeneration can provide valuable insight into the degenerative process in SCA10 and its relationship with the symptoms.

2. Methods

2.1. Participants

Eighteen patients belonging to 8 families with a confirmed molecular diagnosis of SCA10 participated in this study (9 female, 9 male; all right-handed; mean age/SD, 49/8.8 years). Ataxia severity was measured using the Scale for the Assessment and Rating of Ataxia (SARA) [13]. The SARA is an eight-item scale that tests gait, stance, sitting, and speech, as well as the finger-chase test, finger-nose test, fast alternating movements, and heel-shin test; where higher scores reflect greater impairment. The control group consisted of 18 healthy volunteers matched for age and sex to the SCA10 group (see Table 1 for demographic information and esupp Fig. 1 for pedigree structure, and clinical and molecular characteristics). All study procedures were conducted with the approval of and in accordance with the ethical standards of the committees on human experimentation of the Universidad Nacional Autónoma de México and the Instituto Nacional de Neurología y Neurocirugía Manuel Velasco Suárez. All participants provided informed consent before engaging in the research project.

Table 1
Demographic, clinical and genetic features of the eighteen study participants with SCA10.

	SCA10 patients n = 18	Healthy controls n = 18
Age, years (mean ± SD)	49.2 ± 8.9	55.6 ± 10.7
Gender F:M	9:9	9:9
Disease duration (mean ± SD)	19.8 ± 7.6	n/a
Disease onset (mean ± SD)	31.5 ± 5.9	n/a
SARA score (mean ± SD)	19.4 ± 6.7	n/a
Seizures, n(%)	11 (61.0%)	n/a
(ATTCT)n range	1610–3800	n/a

SARA: Scale for the Assessment and Rating of Ataxia[22]; F: Female; M: Male. Exp: (ATTCT)n repeat in pathogenic, expanded range; n/a: not applicable.

2.2. Image acquisition

All images were acquired using a 3 T Achieva MRI scanner (Phillips Medical Systems, Eindhoven, The Netherlands) at the Instituto Nacional de Psiquiatría Ramón de la Fuente Muñiz in Mexico City. The high-resolution anatomical acquisition consisted of a 3-D T1 Fast Field-Echo sequence, with TR/TE of 8/3.7 m s, FOV of 256 × 256 mm, and an acquisition and reconstruction matrix of 256 × 256, resulting in an isometric resolution of 1 × 1 × 1 mm. The DTI sequences consisted of Single Shot Echo Planar Imaging sequences, acquiring 33 vol of 70 axial slices (2 mm slice thickness and no separation), one for each of the 32 independent directions of diffusion with b = 800 s/mm2 and one corresponding to b = 0 s/mm2, TR/TE = 8467/60 m s, FOV 256 × 256 mm2 and an acquisition and reconstruction matrix of 128 × 128, resulting in an isometric resolution of 2 × 2 × 2 mm3.

2.3. Tract-Based Spatial Statistics

Diffusion images were processed using FSL's Diffusion Toolbox (FMRIB's Software Library, www.fmrib.ox.ac.uk/fsl) [14]. Eddy current effects were corrected and the diffusion tensor model was adjusted to generate the fractional anisotropy maps for each participant. The statistical analysis was done in a voxel-wise manner using the Tract-Based Spatial Statistics methodology [15]. A two-sample *t*-test between the SCA10 and the control group was performed for fractional anisotropy (FA) using FSL's randomise. Age was included as covariate of no interest. Correction for multiple comparisons was assessed using randomized permutation methods. Only those voxels surviving this correction at a p value < 0.05 were considered as showing a significant group difference.

2.4. voxel-based morphometry

Gray matter volume measurements were performed using voxel-based morphometry (VBM) as implemented on FSL following the standard procedure [16]. Using the FSL randomise tool, a two-sample *t*-test was performed between the SCA10 group and controls. Since prior studies using imaging measures have described age-associated changes across the cerebral cortex [17] we included the age data in the model as variable of no interest. Significance was defined as $p < 0.05$ after correcting for multiple comparisons using the randomized permutation method [18].

2.5. Associations between the degeneration and clinical scores

To find associations between the degeneration and the clinical scores, we used two approaches: a) for the FA we computed the average value of a 6 mm sphere centered at the local maxima of each significant cluster from the group comparison; b) for the GM we used the voxels included in the significant group differences. Then we calculated the

correlation between the imaging values and the SARA score, as well as, the presence of seizures (after controlling for the age). Due to the binary nature of the presence of seizures, we performed a *t*-test between patients with and without seizures. For visualization purposes, the data is presented as scatter or box plots next to the corresponding MRI images.

2.6. Degeneration signature

VBM is a powerful tool to investigate the grey matter degeneration in patients compared to healthy subjects; however, the resulting parametric map shows brain areas in which the intensity of the grey matter is significantly different between groups. These VBM maps are useful to reveal all brain areas that are affected in a particular cohort, but they are skewed by patients with larger amounts of degeneration obscuring the primary target of the disease at the early stage. The degeneration signature normalizes the amount of degeneration of each patient controlling by his/her overall amount of cerebellar damage, thus penalizing patients with a large amount of degeneration. The resulting average degeneration map reveals the underlying pattern at the initial stage, making it possible to differentiate between different subtypes of SCAs [12]. The degeneration signature analysis was performed using MATLAB 2018b (The Mathworks, Inc Natick, MA). In summary, the following analysis steps were taken: isolation of the cerebellum from the rest of the brain, normalization to the SUIT template [19], adjustment of the intensity of the cerebellar grey matter based on brain size, estimation of the mean degeneration of each patient, and computation of the average of the corrected grey matter maps. For further details, see Hernandez-Castillo et al. [12]. All analyses were computed within the volume, but for visualization purposes, the data was projected into the SUIT flatmap [20].

3. Results

In order to expand the current knowledge of the degenerative process of SCA10, we used VBM and TBSS to systematically assess whole-brain abnormalities and the SUIT toolbox to further analyze the cerebellar cortex. We also explored associations between the structural measurements and the clinical scores.

3.1. Tract-based spatial statistics

TBSS group comparison revealed significant FA decreases in SCA10 patients (Fig. 1A and esupp Table 1). No significant increases were found in the patients. Further analyses found associations between the patient's SARA score and the FA in the right cerebellar lobule VI ($r = -0.45$, $p = 0.049$; $x = 15$, $y = -64$, $z = -33$; Fig. 1B) in which patients with lower FA values had higher SARA score. No other correlations with the SARA score were found. We also found an association between the presence of seizures and the FA of the cerebellar lobule V ($x = -6$, $y = -56$, $z = -20$; Fig. 1C) in which patients that have not presented seizures have higher FA values compared to those that had seizures ($t = 2.82$, $p = 0.012$).

3.2. Voxel-based morphometry

The VBM group comparison revealed significant grey matter decreases in the cerebellum, brainstem, thalamus, putamen, cingulate and precentral gyrus (Fig. 1D and esupp Table 2) in SCA10 patients in comparison to controls. No significant increases were found in the patient group. The degeneration signature map showed that the grey matter atrophy in the cerebellum is more prevalent in parts of lobules VIIIb, IX, and X (Fig. 1F). We found associations between the grey matter intensity and the SARA score in a number of cerebellar regions (Fig. 2A), including lobules V($x = 7$, $y = -57$, $z = -10$; $r = -0.84$, $p < 0.001$), VI ($x = -34$, $y = -44$, $z = -30$; $r = -0.83$, $p < 0.001$), left IX ($x = -5$, $y = -54$, $z = -56$; $r = -0.75$, $p < 0.001$), and right IX ($x = 7$, $y = -60$, $z = -52$; $r = -0.79$, $p < 0.001$), as well as in the vermis VIIIa ($x = -1$, $y = -67$, $z = -33$; $r = -0.76$, $p < 0.001$). Patients with lower grey matter intensity in those cerebellar areas had higher SARA scores. No other correlations with the SARA score were found. Thalamic degeneration was associated with the presence of seizures (Fig. 2B), where patients without seizures showed higher grey matter intensity compared to those with a history of seizures. This difference was higher in the left ($x = -14$, $y = -12$, $z = 10$; $t = 3.5$, $p = 0.002$) than in the right thalamus ($x = 16$, $y = 28$, $z = 2$; $t = 2.5$, $p = 0.025$).

4. Discussion

This study is a comprehensive analysis of grey and white matter degeneration and how it relates to the clinical features in a cohort of SCA10 patients. The results show significant white matter deterioration in the cerebellum, brainstem, thalamus, putamen, cingulate, and precentral gyrus. There are no previous reports of the patterns of brain neurodegeneration in sizable groups of SCA10 patients to compare our findings to, but a post-mortem neuropathological study of one patient autopsy revealed significant degeneration of the Purkinje cells of the cerebellum [5]. The results from our unbiased pattern of degeneration analysis suggest that the cerebellar degeneration starts in the posterior/floculonodular cerebellum. As expected, the relationship between neurodegeneration and clinical profile shows an inverse association between cerebellar integrity and ataxia severity, as measured on the SARA scale. Additionally, patients with seizures had significant lower grey matter intensity in the thalamus and loss of integrity of the white matter in the lobule VI of the cerebellum. Following is a discussion of these findings.

4.1. White matter abnormalities

TBSS analysis reveals reduced FA of the white matter tracts in the cerebellum but not in other regions. The FA values were lower in the anterior cerebellum, which is consistent with reports of other SCA subtypes including SCA1, SCA2, SCA3, and SCA7 [21,22]; however, in all those subtypes the abnormalities of the white matter extend to the brainstem and the cerebral cortex at different levels. These reductions of the FA values imply disease-related microstructural changes in the afferent and efferent projections of the cerebellum. Furthermore, the combination of white matter degeneration and gray matter loss in the cerebellum results in a variety of clinical motor impairments, including ataxia and extrapyramidal signs [23]. We found an association between the ataxia severity and the FA values in the anterior cerebellum, which included the anterior thalamic radiation and the corticospinal tract. The degeneration of these main tracts affects the information flow between the cerebellum and the motor and frontal cortices, which might result in the loss of coordination and dexterity in this set of patients. Furthermore, we found that SCA10 patients that have seizures also have lower FA values in areas of lobule VI including the corticospinal tract. Reduction of the white matter integrity has been reported in different epileptic disorders, including a significant change of FA in patients with temporal lobe [24] and idiopathic-generalized epilepsy [25]. Although our results show evidence of the association between the white matter integrity and the presence of seizures, further comprehensive studies might clarify the level of involvement of these structural abnormalities and the epileptic episodes.

4.2. Grey matter abnormalities

As expected, VBM revealed degeneration of the cerebellum and brainstem. Further analysis found associations between the degeneration in the anterior regions of the cerebellum and the motor impairment. The anterior lobule of the cerebellum, which communicates with the motor and premotor cortices via the thalamus, is commonly

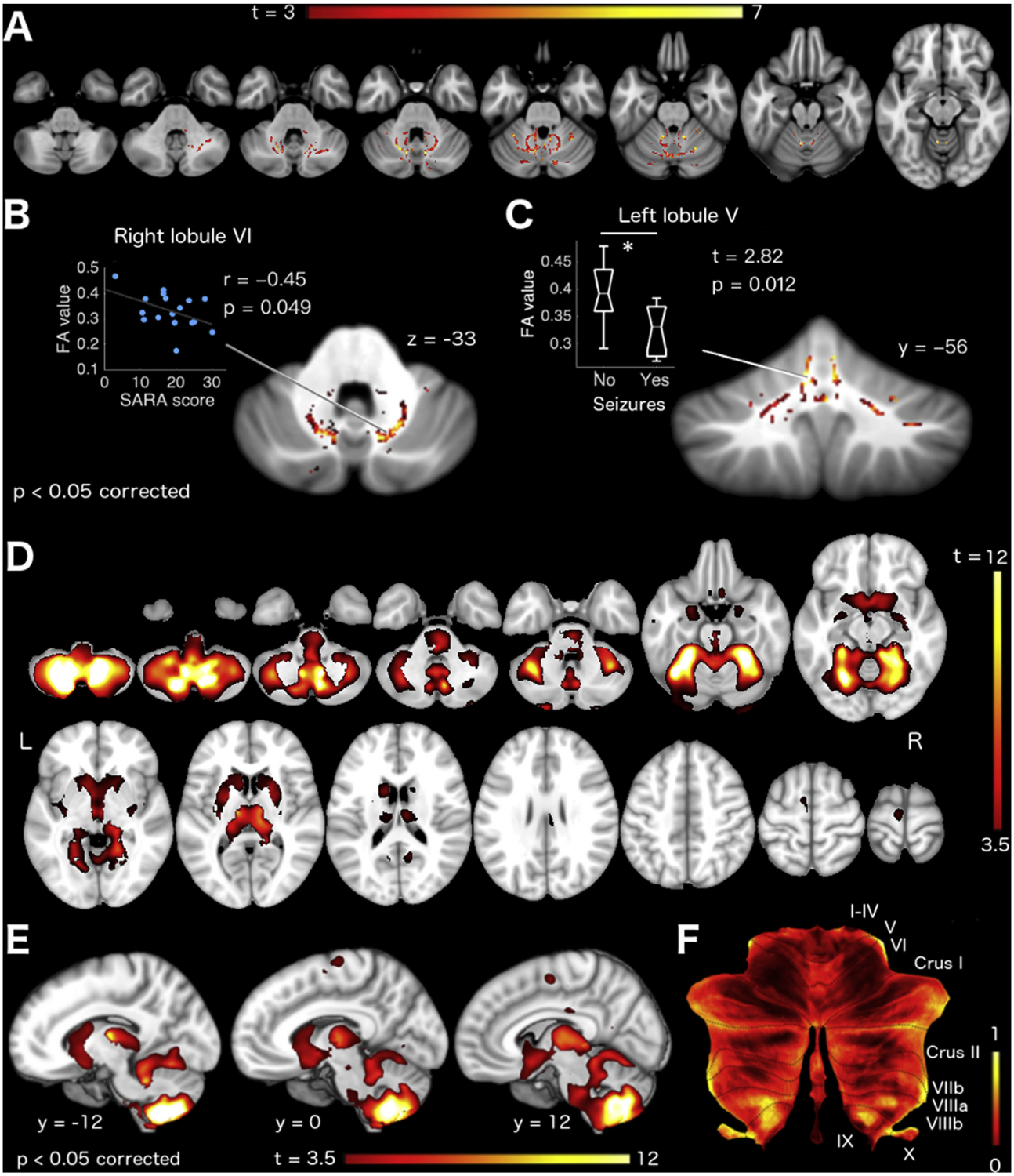

Fig. 1. Structural abnormalities. A) TBSS group comparison between SCA10 patients and healthy controls. Warm colors indicate the white matter tracts showing a significant decrease of the fractional anisotropy in the SCA10 patients. B) Axial section of the cerebellum showing the area in which we found a significant association between SARA score and the FA of the thalamic radiation. The scatter plot shows the FA value per patient in the local maxima. C) Coronal section of the cerebellum showing the area in which we found an association between the presence of seizures and the FA of the corticospinal tract. The bar plot shows the grey matter intensity of SCA10 patients with and without seizures. D) Axial sections showing VBM group comparison between SCA10 and healthy controls. Warm colors indicate the regions with a significant decrease of the gray matter intensity in SCA10 patients. E) Sagittal sections of D. F) Degeneration signature of SCA10 in a flat representation of the cerebellar cortical sheet. Warm colors indicate the unbiased degeneration intensity. (For interpretation of the references to color in this figure legend, the reader is referred to the Web version of this article.)

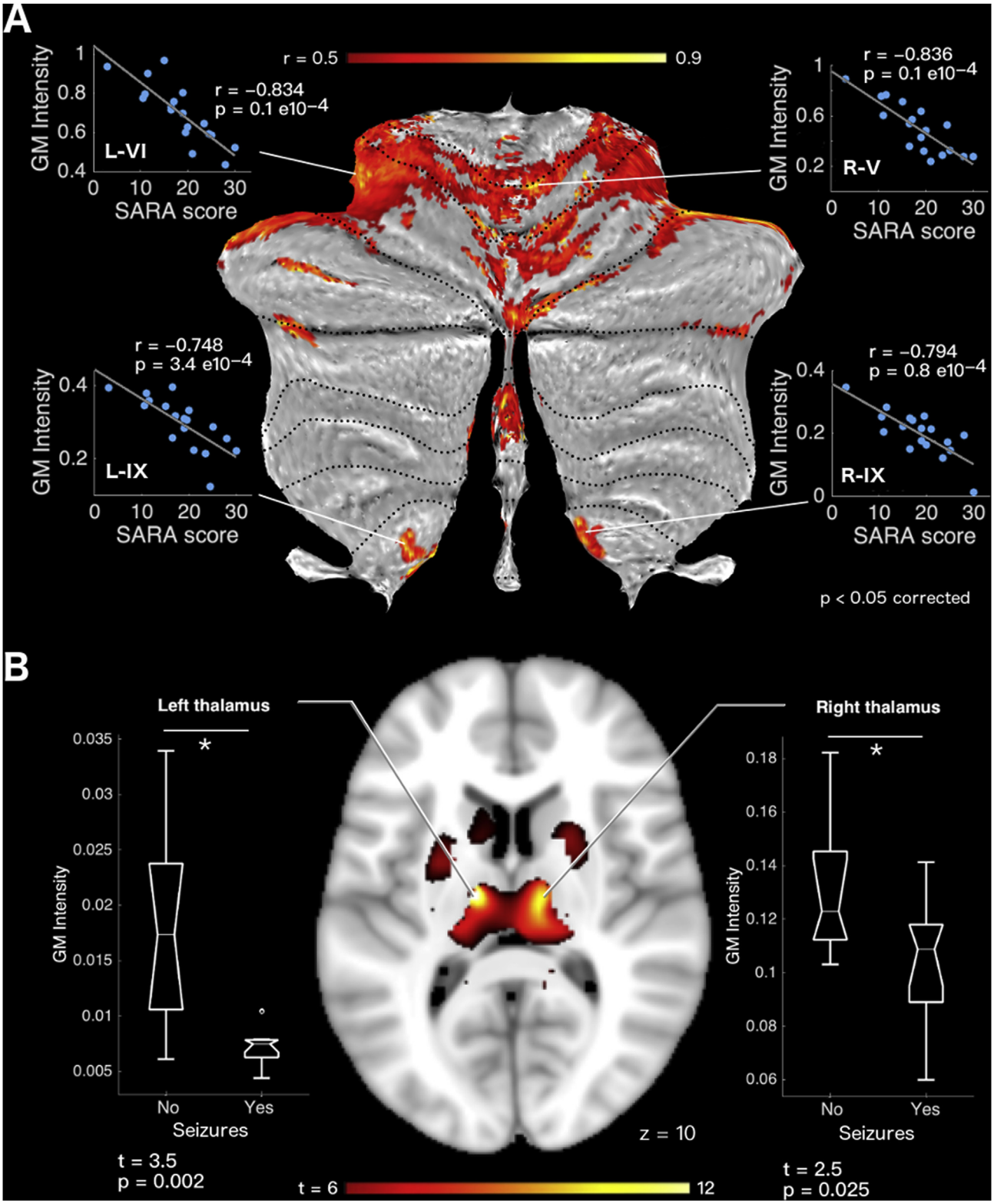

Fig. 2. Associations between gray matter volume and clinical scores. A) Associations between SARA and VBM grey matter intensity. Warm colors indicate the cerebellar regions showing significant inverse associations. Scatter plots show the grey matter intensity value per patient in the higher local maxima. B) Associations between seizures presence and VBM grey matter intensity. Warm colors indicate the regions showing a significant decrease of the gray matter intensity in SCA10 patients in comparison to healthy controls. The bar plots show the grey matter intensity of SCA10 patients with and without seizures. Note the large association between seizure presence and gray matter intensity in the bilateral thalamus. (For interpretation of the references to color in this figure legend, the reader is referred to the Web version of this article.)

degenerated in a number of SCAs, and it is usually associated with motor impairment in these diseases [12]. The VBM analysis also showed decreased grey matter in the thalamus, putamen, cingulate, and precentral gyrus, suggesting that the SCA10 degenerative process is not confined to the cerebellum and brainstem. Extra-cerebellar degeneration is usually present in different SCA subtypes [26]. For example, cingulate and precentral gyrus degeneration has been reported in SCA1, SCA2, SCA3, SCA7, and SCA17 [22,27,28]. Nonetheless, despite the thalamus showing the highest degeneration after the cerebellum, the analysis did not find any association between the thalamic grey matter intensity and the degree of motor impairment. On the other hand, our results did show that patients with a history of seizures showed more thalamic degeneration compared to those patients that have not presented seizures. The thalamus and basal ganglia play important roles in controlling seizure activity throughout the brain, regardless of the location of the epileptogenic focus [29], epileptic seizures are common in patients with medial thalamic lesions [30]. Similar thalamic degeneration has been reported in individual cases or small groups of SCA17 and DRPLA patients that presented seizures [31]. However, due to a lack of a systematic assessment of the degeneration, these visual inspections do not allow a direct comparison with our results. Overall, the association between the thalamic degeneration and the presence of seizures in our cohort of SCA10 patients is consistent with the literature; however, as in other epileptic disorders, it is uncertain whether the thalamic lesion is the cause or the consequence of the epileptic activity [30].

The precise mechanisms of neurodegeneration in most SCAs, including SCA10, are currently unknown. The SCA10 pentanucleotide repeat expansion is an RNA-mediated gain of function mutation. Initially, it was thought that the mutation resulted in a loss of function, given that the product of the gene, Ataxin 10, is required for neuronal survival and may induce outgrowth when overexpressed; however, ATXN10 transcript levels in SCA10 patients are similar to levels in normal controls [31]. The intron containing the (ATTCT)n repeat is spliced out during transcription both in the normal and expanded range, but when the RNA contains (AUUCU) repeats in the pathogenic range, the repeat aggregates and sequesters hnRNP K, which in turns leads to apoptosis in specific neuronal subpopulations [32]. SCA10 mouse models replicating these intra-cytoplasmic aggregates have shown neuronal loss in the hippocampus, cerebral cortex and pontine nuclei and a clinical phenotype reminiscent of SCA10 with seizures [32]. The one autopsy case of a human patient with SCA10 revealed extensive degeneration and loss of Purkinje cells with early dendritic degeneration. Additional dendritic atrophy in the dentate nucleus and neuronal loss in the inferior olivary nuclei were suggested to be a result of retrograde neuronal loss secondary to the extensive Purkinje cell degeneration [33].

4.3. Degeneration signature

The VBM group analysis revealed intense degeneration in the anterior cerebellum including areas of lobules I-VI and posterior areas in lobule VIII-X. The main difference between the VBM and the degeneration signature analyses presented herein is, that by controlling for the severity of the degeneration, the resulting map shows the areas that are implicated in all patients, regardless of the disease severity or progression. Therefore, this analysis provides an informed estimate of the initial pattern of degeneration [12]. After the correction for the degeneration severity, the area that showed the most degeneration included lobules VIII-X. This area of the cerebellum has been also associated with motor control, and lesions due to posterior inferior cerebellar artery stroke result in balance, gait and limb ataxia [30]. Furthermore, other SCA subtypes analyzed with this technique have also shown degeneration in lobules IX and X [12]. In comparison, the degeneration pattern in SCA10 seems to have communalities with SCA2, SCA3 and SCA7 in the posterior lobule of the cerebellum. However, SCA10 patients also showed involvement of the crus 1, which is not observed in the other SCA subtypes. Thus, based on our results we can suggest that the anterior cerebellar degeneration in SCA10 starts later in the degenerative process. While the exact mechanisms through which the SCA10 mutation leads to clinical disease remain unclear, the degeneration signatures point to areas containing cellular subpopulations that are particularly susceptible to the suggested RNA-mediated toxicity of the mutant Ataxin 10.

4.4. Strengths and limitations

We did not include the number of ATTCT repeats in our analyses because SCA10 expansions are very difficult to accurately quantify and repeat sizes are often estimated rather than precise numbers. In this cohort, all subjects identified as SCA10 patients had a proven (ATTCT) repeat within the expanded range, but the specific number of repeats was not determined in all cases. Furthermore, the detailed features of the seizures in terms of type, electroencephalographic characteristics, frequency, and response to treatment were not available for all patients. Therefore, seizures were included in the analysis only as a dichotomous variable (present vs. absent). Future studies would gain from correlations with specific features of the seizure phenotype.

The sample size of this study is large for a disease considered very rare, but all our cases are of Mexican origin and several of them belong to the same family. Future studies including larger populations of diverse origins will enrich the characterization of the degenerative process. This is particularly relevant given that there seem to be two subphenotypes of SCA10: the “Mexican SCA10”, also observed in Argentina, Venezuela, Peru and some areas of Brazil and which is characterized by high rates of epilepsy; and the originally named “Brazilian SCA10”, affecting a large number of families in the southern Brazilian states of Santa Catarina and Parana, who only exceptionally have seizures [4,9]. Collaborative initiatives between international health centers and research institutes can make a difference in this regard.

In conclusion, our systematic characterization of the brain degeneration in SCA10 shows specific brain regions where the white or grey matter degeneration correlates with the severity of ataxia, all of which are closely related to the movement coordination problems displayed by SCA10 patients. We also showed that thalamic degeneration could be associated with the presence of seizures. These findings contribute to a better understanding of the neural basis of the symptomatology presented by patients with SCA10.

Appendix A. Supplementary data

Supplementary data to this article can be found online at https://doi.org/10.1016/j.parkreldis.2019.08.011.

Author contributions

CHC and JFR, conceived and designed the study; CHC, RD, IVP, DLT, AC, ACR, AO, AR contributed to the acquisition and analysis of the data, and CHC, AR and JFR participated in the drafting and final approval of the manuscript.

Potential conflicts of interest

All authors have no conflict of interest to disclose.

Funding

This work was funded by UNAM grant DGAPA-PAPIIT No. IN220019, CONACYT A1-S-10669 to JFR and CONACYT PhD scholarship 697735 to AC.

References

[1] T. Matsuura, T. Yamagata, D. Burgess, A. Rasmussen, R. Grewal, K. Watase, M. Khajavi, A. McCall, C. Davis, L. Zu, M. Achari, S. Pulst, E. Alonso, J. Noebels, D. Nelson, H. Zoghbi, T. Ashizawa, Large expansion of the ATTCT pentanucleotide repeat in spinocerebellar ataxia type 10, Nat. Genet. 26 (2) (2000) 191–194.

[2] A. Rasmussen, T. Matsuura, L. Ruano, P. Yescas, A. Ochoa, T. Ashizawa, E. Alonso, Clinical and genetic analysis of four Mexican families with spinocerebellar ataxia type 10, Ann. Neurol. 50 (2) (2001) 234–239.

[3] E.M. Gatto, R. Gao, M.C. White, M.C. Uribe Roca, J.L. Etcheverry, G. Persi, J.J. Poderoso, T. Ashizawa, Ethnic origin and extrapyramidal signs in an Argentinean spinocerebellar ataxia type 10 family, Neurology 69 (2) (2007) 216–218.

[4] H.A. Teive, R.P. Munhoz, W.O. Arruda, S. Raskin, L.C. Werneck, T. Ashizawa, Spinocerebellar ataxia type 10 - a review, Park. Relat. Disord. 17 (9) (2011) 655–661.

[5] K. Bushara, M. Bower, J. Liu, K.N. McFarland, I. Landrian, D. Hutter, H.A. Teive, A. Rasmussen, C.J. Mulligan, T. Ashizawa, Expansion of the Spinocerebellar ataxia type 10 (SCA10) repeat in a patient with Sioux Native American ancestry, PLoS One 8 (11) (2013) e81342.

[6] H. Naito, T. Takahashi, M. Kamada, H. Morino, H. Yoshino, N. Hattori, H. Maruyama, H. Kawakami, M. Matsumoto, First report of a Japanese family with spinocerebellar ataxia type 10: the second report from Asia after a report from China, PLoS One 12 (5) (2017) e0177955.

[7] L. Leonardi, C. Marcotulli, K.N. McFarland, A. Tessa, R. DiFabio, F.M. Santorelli, F. Pierelli, T. Ashizawa, C. Casali, Spinocerebellar ataxia type 10 in Peru: the missing link in the Amerindian origin of the disease, J. Neurol. 261 (9) (2014) 1691–1694.

[8] H.A. Teive, B.B. Roa, S. Raskin, P. Fang, W.O. Arruda, Y.C. Neto, R. Gao, L.C. Werneck, T. Ashizawa, Clinical phenotype of Brazilian families with spinocerebellar ataxia 10, Neurology 63 (8) (2004) 1509–1512.

[9] H.A. Teive, A. Moro, M. Moscovich, W.O. Arruda, R.P. Munhoz, S. Raskin, G.M. Teive, N. Dallabrida, T. Ashizawa, Spinocerebellar ataxia type 10 in the South of Brazil: the Amerindian-Belgian connection, Arq. Neuro. Psiquiatr. 73 (8) (2015) 725–727.

[10] V.P. Cintra, C.M. Lourenco, S.E. Marques, L.M. de Oliveira, V. Tumas, W. Marques Jr., Mutational screening of 320 Brazilian patients with autosomal dominant spinocerebellar ataxia, J. Neurol. Sci. 347 (1–2) (2014) 375–379.

[11] L. Schöls, P. Bauer, T. Schmidt, T. Schulte, O. Riess, Autosomal dominant cerebellar ataxias: clinical features, genetics, and pathogenesis, Lancet Neurol. 3 (5) (2004) 291–304.

[12] C.R. Hernandez-Castillo, M. King, J. Diedrichsen, J. Fernandez-Ruiz, Unique degeneration signatures in the cerebellar cortex for spinocerebellar ataxias 2, 3, and 7, Neuroimage Clin 20 (2018) 931–938.

[13] S.H. Subramony, SARA–a new clinical scale for the assessment and rating of ataxia, Nature clinical practice, Neurology 3 (3) (2007) 136–137.

[14] S.M. Smith, M. Jenkinson, M.W. Woolrich, C.F. Beckmann, T.E. Behrens, H. Johansen-Berg, P.R. Bannister, M. De Luca, I. Drobnjak, D.E. Flitney, R.K. Niazy, J. Saunders, J. Vickers, Y. Zhang, N. De Stefano, J.M. Brady, P.M. Matthews, Advances in functional and structural MR image analysis and implementation as FSL, Neuroimage 23 (Suppl 1) (2004) S208–S219.

[15] S.M. Smith, M. Jenkinson, H. Johansen-Berg, D. Rueckert, T.E. Nichols, C.E. Mackay, K.E. Watkins, O. Ciccarelli, M.Z. Cader, P.M. Matthews, T.E. Behrens, Tract-based spatial statistics: voxelwise analysis of multi-subject diffusion data, Neuroimage 31 (4) (2006) 1487–1505.

[16] J. Ashburner, K.J. Friston, Voxel-based morphometry–the methods, Neuroimage 11 (6 Pt 1) (2000) 805–821.

[17] N. Raz, F.M. Gunning, D. Head, J.H. Dupuis, J. McQuain, S.D. Briggs, W.J. Loken, A.E. Thornton, J.D. Acker, Selective aging of the human cerebral cortex observed in vivo: differential vulnerability of the prefrontal gray matter, Cerebr. Cortex 7 (3) (1997) 268–282.

[18] S. Hayasaka, T.E. Nichols, Combining voxel intensity and cluster extent with permutation test framework, Neuroimage 23 (1) (2004) 54–63.

[19] J. Diedrichsen, A spatially unbiased atlas template of the human cerebellum, Neuroimage 33 (1) (2006) 127–138.

[20] J. Diedrichsen, E. Zotow, Surface-based display of volume-averaged cerebellar imaging data, PLoS One 10 (7) (2015) e0133402.

[21] J.B. Schulz, J. Borkert, S. Wolf, T. Schmitz-Hubsch, M. Rakowicz, C. Mariotti, L. Schols, D. Timmann, B. van de Warrenburg, A. Durr, M. Pandolfo, J.S. Kang, A.G. Mandly, T. Nagele, M. Grisoli, R. Boguslawska, P. Bauer, T. Klockgether, T.K. Hauser, Visualization, quantification and correlation of brain atrophy with clinical symptoms in spinocerebellar ataxia types 1, 3 and 6, Neuroimage 49 (1) (2010) 158–168.

[22] C.R. Hernandez-Castillo, V. Galvez, R. Diaz, J. Fernandez-Ruiz, Specific cerebellar and cortical degeneration correlates with ataxia severity in spinocerebellar ataxia type 7, Brain Imaging Behav 10 (1) (2016) 252–257.

[23] W. Fries, A. Danek, K. Scheidtmann, C. Hamburger, Motor recovery following capsular stroke. Role of descending pathways from multiple motor areas, Brain : J. Neurol. 116 (Pt 2) (1993) 369–382.

[24] R.M. Govindan, M.I. Makki, S.K. Sundaram, C. Juhasz, H.T. Chugani, Diffusion tensor analysis of temporal and extra-temporal lobe tracts in temporal lobe epilepsy, Epilepsy Res. 80 (1) (2008) 30–41.

[25] N.K. Focke, C. Diederich, G. Helms, M.A. Nitsche, H. Lerche, W. Paulus, Idiopathic-generalized epilepsy shows profound white matter diffusion-tensor imaging alterations, Hum. Brain Mapp. 35 (7) (2014) 3332–3342.

[26] A.M. Duenas, R. Goold, P. Giunti, Molecular pathogenesis of spinocerebellar ataxias, Brain : J. Neurol. 129 (Pt 6) (2006) 1357–1370.

[27] G. Goel, P.K. Pal, S. Ravishankar, G. Venkatasubramanian, P.N. Jayakumar, N. Krishna, M. Purushottam, J. Saini, M. Faruq, M. Mukherji, S. Jain, Gray matter volume deficits in spinocerebellar ataxia: an optimized voxel based morphometric study, Park. Relat. Disord. 17 (7) (2011) 521–527.

[28] C.R. Hernandez-Castillo, R. Diaz, A. Campos-Romo, J. Fernandez-Ruiz, Neural correlates of ataxia severity in spinocerebellar ataxia type 3/Machado-Joseph disease, Cerebellum Ataxias 4 (2017) 7.

[29] S. Dreifuss, F.J. Vingerhoets, F. Lazeyras, S.G. Andino, L. Spinelli, J. Delavelle, M. Seeck, Volumetric measurements of subcortical nuclei in patients with temporal lobe epilepsy, Neurology 57 (9) (2001) 1636–1641.

[30] S.S. Keller, M.P. Richardson, J. O'Muircheartaigh, J.C. Schoene-Bake, C. Elger, B. Weber, Morphometric MRI alterations and postoperative seizure control in refractory temporal lobe epilepsy, Hum. Brain Mapp. 36 (5) (2015) 1637–1647.

[31] M. Wakamiya, T. Matsuura, Y. Liu, G.C. Schuster, R. Gao, W. Xu, P.S. Sarkar, X. Lin, T. Ashizawa, The role of ataxin 10 in the pathogenesis of spinocerebellar ataxia type 10, Neurology 67 (4) (2006) 607–613.

[32] M. White, G. Xia, R. Gao, M. Wakamiya, P.S. Sarkar, K. McFarland, T. Ashizawa, Transgenic mice with SCA10 pentanucleotide repeats show motor phenotype and susceptibility to seizure: a toxic RNA gain-of-function model, J. Neurosci. Res. 90 (3) (2012) 706–714.

[33] G. Xia, K.N. McFarland, K. Wang, P.S. Sarkar, A.T. Yachnis, T. Ashizawa, Purkinje cell loss is the major brain pathology of spinocerebellar ataxia type 10, J. Neurol. Neurosurg. Psychiatry 84 (12) (2013) 1409–1411.